390–400 *Nucleic Acids Research, 2007, Vol. 35, No. 2* *Published online 14 December 2006*
doi:10.1093/nar/gkl1052

Association of Dnmt3a and thymine DNA glycosylase links DNA methylation with base-excision repair

Ya-Qiang Li[1,2], Ping-Zhu Zhou[1,2], Xiu-Dan Zheng[1,2], Colum P. Walsh[3] and Guo-Liang Xu[1,*]

[1]The State Key Laboratory of Molecular Biology, Institute of Biochemistry and Cell Biology, Shanghai Institutes for Biological Sciences, Chinese Academy of Sciences, [2]Graduate School of Chinese Academy of Sciences, 320 Yueyang Road, Shanghai 200031, China and [3]Centre for Molecular Biosciences, School of Biomedical Sciences, University of Ulster BT52 1SA, Northern Ireland, UK

Received June 2, 2006; Revised November 16, 2006; Accepted November 17, 2006

ABSTRACT

While methylcytosines serve as the fifth base encoding epigenetic information, they are also a dangerous endogenous mutagen due to their intrinsic instability. Methylcytosine undergoes spontaneous deamination, at a rate much higher than cytosine, to generate thymine. In mammals, two repair enzymes, thymine DNA glycosylase (TDG) and methyl-CpG binding domain 4 (MBD4), have evolved to counteract the mutagenic effect of methylcytosines. Both recognize G/T mismatches arising from methylcytosine deamination and initiate base-excision repair that corrects them to G/C pairs. However, the mechanism by which the methylation status of the repaired cytosines is restored has remained unknown. We show here that the DNA methyltransferase Dnmt3a interacts with TDG. Both the PWWP domain and the catalytic domain of Dnmt3a are able to mediate the interaction with TDG at its N-terminus. The interaction affects the enzymatic activity of both proteins: Dnmt3a positively regulates the glycosylase activity of TDG, while TDG inhibits the methylation activity of Dnmt3a *in vitro*. These data suggest a mechanistic link between DNA repair and remethylation at sites affected by methylcytosine deamination.

INTRODUCTION

DNA cytosine methylation is a common and rapidly evolving epigenetic mechanism among higher eukaryotic organisms with more complex genomes (1). In mammalian genomes, 5% of the cytosines are methylated. Methylcytosines occur predominantly at CpG dinucleotides. DNA methylation is essential for normal development due to its important roles in genomic imprinting, X chromosome inactivation, silencing of parasitic elements, regulation of tissue-specific gene expression and the maintenance of heterochromatin (2,3). The distribution of methylated and unmethylated CpGs in genomic DNA is not random, but displays specific patterns in any given type of cell (4,5). The generation of genomic methylation patterns is a dynamic process that requires demethylation and *de novo* methylation by the action of the two *de novo* methyltransferases, Dnmt3a and Dnmt3b, during gametogenesis and early embryonic development (6). Once the methylation patterns are created, they are perpetuated by the maintenance methyltransferase Dnmt1, leading to somatic inheritance (2). Aberrant methylation is known to contribute to tumorigenesis and other diseases (7–9).

However, methylcytosines are also a source of genomic instability because they are prone to hydrolytic deamination under physiological conditions. The deamination product of a methylcytosine is thymine, a naturally occurring base. If the mispaired thymine is not repaired, a C to T transition will be fixed following DNA replication. Since methylcytosines exist in large numbers throughout the mammalian genome (3×10^7 per haploid genome), they present a significant risk for mutagenesis. The mutation rate from methylcytosine to thymine is 10- to 50-fold higher than for other types of transitions (10,11). One-third of all germ-line point mutations found in human diseases and an equal proportion of somatic mutations associated with cancer occur at CpG sites (12,13). The methylated CpG sites in the tumor suppressor gene p53 are, for example, hot spots for mutation in carcinogenesis (14,15).

In mammals, a specific base-excision repair pathway is devoted to the correction of G/T mismatches arising due to methylcytosine deamination (16,17). The repair process is initiated by a DNA glycosylase, either thymine DNA glycosylase (TDG) or methyl-CpG binding domain 4 (MBD4), that recognizes and excises the mispaired thymine from the ribose

*To whom correspondence should be addressed. Tel: +86 21 5492 1332; Fax: +86 21 5492 1333; Email: glxu@sibs.ac.cn

The authors wish it to be known that, in their opinion, the first two authors should be regarded as joint First Authors

ring, generating an abasic residue (18–20). At the abasic site, a single nucleotide gap is then created by apurinic/apyrimidinic endonuclease (APE, also known as HAP1, APEX and Ref-1) that cleaves the phosphodiester bond 5′ of the baseless deoxyribose. The APE–DNA complex is then channeled into an appropriate base-excision repair (BER) pathway (21). The repair is completed by the concerted action of DNA polymerase β (POLB), XRCC1 and DNA ligase III (LIG3), which results in the replacement of the missing nucleotide and the establishment of the continuity of the DNA strand (16). The question then arises as to how the original methylation state is restored to the cytosine left by base-excision repair. It was reported that cytosine incorporated by DNA repair is remethylated in a replication-independent manner (22), but the molecular mechanism remains to be elucidated. In this study we demonstrate that Dnmt3a interacts with TDG both *in vitro* and *in vivo*. Functional assays with recombinant proteins indicate that Dnmt3a stimulates the TDG glycosylase activity whereas in turn TDG inhibits the methylation activity of Dnmt3a. The physical and functional interaction with TDG suggests that Dnmt3a might be the enzyme that remethylates the newly synthesized cytosine to ensure stable maintenance of methylation after base-excision repair.

MATERIALS AND METHODS

Plasmid constructs

Mouse TDG was cloned into the expression vector pFLAG-CMV-2 (Sigma) and pCMV-Tag3C (Stratagene) to generate Flag- and myc-tagged proteins, respectively. Full-length human APE, POLB, XRCC1 and LIG3 were cloned into a modified pCDNA4 vector in-frame with the Flag tag at the N-terminus. The full-length coding region and various subregions of TDG were cloned into pET28a (Novagen) and pGADT7 (Clontech) for *in vitro* expression and yeast two-hybrid assay. We verified all PCR-cloned constructs by DNA sequencing.

Cell culture and transfections

Human embryonic kidney HEK 293T, 293 c18 (ATCC no. CRL-10852) and mouse fibroblast NIH 3T3 cells were maintained in DMEM with standard supplements. Plasmid constructs and G/T mismatch-containing DNA oligoduplexes were transfected into the cells using LipofectAMINE (Invitrogen).

Reagents and antibodies

M.HhaI and M.SssI methyltransferases were from NEB. Uracil DNA glycosylase (UDG) and micrococcal nuclease were from Fermentas. The antibody specific for Dnmt3a was raised and affinity-purified as described previously (23). The monoclonal anti-myc and polyclonal anti-HA were from Santa Cruz, monoclonal anti-Flag and anti-HA were from Sigma–Aldrich. The Alexa Fluor® 546 goat anti-rabbit IgG and Alexa Fluor® 488 goat anti-mouse IgG were purchased from Molecular Probes. The goat anti-mouse IgG conjugated with indodicarbocyanine (Cy5) was from Jackson ImmunoResearch.

Yeast two-hybrid assay

Two-hybrid screening was performed by mating a yeast strain construct (AH109) harboring GAL4DB-Dnmt3a with a strain (Y187) carrying a mouse testis expression library (Clontech). Colonies were selected on the SD medium lacking His, Leu, Trp and adenine according to the recommended protocol (Clontech). The prey plasmids from positive clones were isolated and transformed into *Escherichia coli* for identification. For mapping the region of Dnmt3a and TDG involved in the interaction, Dnmt3a fragments were cloned in-frame with GAL4 DNA binding domain (GAL4DB) on the bait vector pGBKT7 (Clontech) and TDG fragments were fused with the GAL4 activation domain (GAL4AD) on the prey vector pGADT7.

Glutathione *S*-transferase (GST) pull-down assay

To confirm the interaction of Dnmt3a and TDG, GST pull-down assay was performed essentially as described (24). A total of 2 μg of the GST–TDG fusion protein purified from bacteria were incubated with glutathione Sepharose 4B beads (Amersham Biosciences) in the binding buffer [20 mM Tris–HCl (pH 7.9), 0.1 M NaCl, 1 mM EDTA, 5 mM $MgCl_2$, 0.1% NP-40, 1 mM DTT, 0.2 mM phenylmethlysulfonyl fluoride (PMSF) and 20% glycerol] in a total volume of 200 μl at 4°C for 2 h. The GST–TDG slurry was washed with the binding buffer containing 1 M NaCl twice and equilibrated with the binding buffer without EDTA twice. After the purified Dnmt3a protein and the GST–TDG slurry were both treated with micrococcal nuclease at a final concentration of 0.1 U/μl at 30°C for 10 min, 500 ng of the Dnmt3a was added to the slurry and incubated at 4°C for another 2 h. The Sepharose beads were vigorously washed five times with the binding buffer, and bound proteins were fractionated by SDS–PAGE and visualized by immunoblotting.

For mapping the interaction domain of TDG or Dnmt3a, 2 μg of the purified GST–Dnmt3a or GST–TDG fusion protein were incubated with glutathione Sepharose 4B beads (Amersham Biosciences) in the binding buffer [20 mM Tris–HCl (pH 7.5), 150 mM NaCl, 1 mM EDTA, 1 mM DTT, 1 μg/ml leupeptin and 1 mM PMSF] in a total volume of 500 μl at 4°C for 2 h. A total of 15 μl of ^{35}S-labeled TDG or Dnmt3a polypeptides synthesized with the *in vitro* transcription/translation system (Promega) were then added to the slurry and incubated at 4°C for another 2 h. The Sepharose beads were vigorously washed five times with the binding buffer containing 0.1% Triton X-100, and bound proteins were fractionated by SDS–PAGE and visualized by autoradiography. *In vitro* translated APE, POLB, XRCC1 and LIG3 were also incubated with GST–Dnmt3a to detect the interaction using the same protocol.

Immunoprecipitation

For the co-immunoprecipitation assay, 5×10^6 of transfected 293T cells were lysed in lysis buffer [50 mM Tris–HCl (pH 7.5), 1 mM EDTA, 150 mM NaCl, 0.8% NP-40, 10% glycerol, 0.5 mg/ml BSA, 1 μg/ml pepstain A, 1 μg/ml leupeptin, 1.7 μg/ml aprotinin and 1 mM PMSF]. Supernatants were incubated with the IP antibody at 4°C for 2 h. Protein A-Sepharose beads (Amersham Biosciences) were added and the mixture was rotated at 4°C for 3 h. Immunoprecipitates

were collected and washed four times with the lysis buffer. Proteins in the immunoprecipitates were analyzed by standard western blotting.

Immunofluorescence

Indirect immunofluorescence staining to study the co-localization of transfected Dnmt3a and TDG in 3T3 cells was carried out as described (23) and images of stained cells were captured with a Nikon fluorescence microscope (E600) and a confocal laser scanning microscope (Leica). The G/T mismatch-containing DNA oligoduplexes used for transfection were prepared by annealing the T-strand oligonucleotide (5′-FAM-AGCTGCGCGCAAT**T**GATCGCCGGAC-GT-3′, 27mer) labeled with FAM (fluorescein) at the 5′ end with an equal molar amount of the G strand oligonucleotide (5′-ACGTCCGGCGATC**G**ATTGCGCGCAGCT-3′, 27mer). The matched FAM-labeled oligoduplexes were prepared by annealing FAM-labeled C-strand oligonucleotide (5′-FAM-AGCTGCGCGCAAT**C**GATCGCCGGACGT-3′, 27mer) with the G strand oligonucleotide. The 26th nucleotide of each strand was modified by phosphorothiate to prevent exonucleolytic degradation within the transfected cells.

Protein expression and purification

The coding sequences of TDG, Dnmt3a were cloned into pGEX4T-3 (Pharmacia) for expression of the GST-fusions in the *E.coli* strain BL21 (DE3). Protein purification from cells induced with 0.5 mM isopropyl-β-D-thiogalactopyranoside (IPTG) at 27°C for 3 h was performed using glutathione Sepharose 4B (Amersham Biosciences) according to the manufacturer's instruction. For GST–TDG, the eluate was dialyzed and loaded again onto a Mono S HR 5/5 cation exchange column (Amersham Biosciences) equilibrated with buffer A [25 mM sodium phosphate (pH 7.0), 0.1 M NaCl, 1 mM EDTA, 10% glycerol, 0.01% Triton X-100, 1 mM DTT and 0.25 mM PMSF]. Bound proteins were eluted with a linear gradient of 0.1–0.8 M NaCl in buffer A. GST–TDG appeared in fractions eluted around 0.5 M NaCl. Purified GST fusion proteins were dialyzed against 20 mM Tris–HCl (pH 7.5), 100 mM NaCl, 1 mM EDTA, 1 mM DTT and 15% glycerol prior to use or storage in aliquots.

For expression and purification of 6xHis-tagged Dnmt3a and TDG, the respective coding sequences were cloned into pET28a (Novagen). His-Dnmt3a was expressed and purified from *E.coli* strain BL21 (DE3) as described (25). 6xHis-TDG was induced at a cell density of 0.7 $A_{600\ nm}$ for 2.5 h at 37°C with 1 mM IPTG and purified with Nickel NTA agarose (Qiagen), followed by chromatography on a Mono S HR 5/5 column using the conditions described above. 6xHis-TDG appeared in fractions eluted around 0.33 M NaCl. Purified enzymes were dialyzed against 20 mM HEPES (pH 7.5), 1 mM EDTA, 1 mM DTT and 15% glycerol prior to use or storage in aliquots.

6xHis-TDG was also purified in two chromatographic steps. After lysis of the cells and removal of cell debris by centrifugation at 20 000 g for 30 min, the soluble protein fraction was loaded onto a 1 ml Hi-Trap Heparin column (Amersham Pharmacia Biotech) equilibrated with Buffer A [25 mM sodium phosphate (pH 7.0), 1 mM EDTA, 10% glycerol, 1 mM DTT and 0.25 mM PMSF]. Bound proteins were eluted with a linear gradient of 0.1–0.8 M NaCl in buffer A. The glycosylase eluted at the beginning of the 600 mM NaCl step. The thymine DNA glycosylase preparation was further purified on a Mono S HR 5/5 column (Amersham Pharmacia Biotech). 6xHis-TDG was loaded in Buffer A containing 100 mM NaCl and then eluted at around 0.33 M NaCl.

6xHis-Dnmt3L, 6xHis-Dnmt2 and 6xHis-APE were expressed in *E.coli* BL21 (DE3) and purified similarly with Nickel NTA agarose (Qiagen) according to the manufacturer's instruction. Recombinant heterochromatin protein HP1 and human glycosylase SMUG1 were purified as GST-fusions according to the recommended protocol (Amersham Biosciences). For SMUG1, the GST tag was removed with Factor Xa protease cleavage.

Glycosylase activity assay

The glycosylase activity of TDG was analyzed with the 'nicking' procedure described previously (26) with modifications in substrate sequence and reaction buffer conditions. The substrate DNA containing a single G/T mismatch was prepared by annealing the T-strand oligonucleotide (5′-AGCTGCGCGC-AATTGATCGCCGGACGT-3′) labeled by [γ-^{32}P]ATP at the 5′ end with an equal molar amount of the G strand oligonucleotide (5′-ACGTCCGGCGATCGATTGCGCGCA-GCT-3′). The nicking reaction by TDG was carried out at 30°C with 10 nM of the substrate DNA in 25 mM HEPES (pH 7.8), 0.5 mM EDTA, 0.5 mM DTT, 0.5 mg/ml BSA as described by Neddermann *et al.* (18) or 25 mM HEPES (pH 7.8), 50 mM NaCl, 2 mM $MgCl_2$, 0.5 mM EDTA, 0.5 mM DTT, 0.5 mg/ml BSA as described by Shimizu *et al.* (27). 6xHis-Dnmt3a, 6xHis-APE, 6xHis-Dnmt2, M.SssI and M.HhaI were added to test their effects, if any, on the TDG activity. Where appropriate, Dnmt3a storage buffer was added to normalize the reaction conditions. To convert the AP sites in the DNA duplex into single-strand breaks, NaOH and EDTA were added to a final concentration of 90 and 10 mM, respectively, and the reaction was heated at 100°C for 5 min. The samples were then resolved on a 20% denaturing polyacrylamide gel followed by autoradiography. Radioactivity of the cleavage product band and the uncleaved substrate band was quantified using the Storm instrument and ImageQuant software (Molecular Dynamics).

The G/U glycosylase activity of TDG, UDG and SMUG1 was measured with the same assay except that a G/U mismatch was incorporated in the place of G/T in the DNA substrate.

In vitro DNA methylation activity assay

DNA methylation activity was determined as described (28). A biotinylated 2.5 kb PCR fragment amplified from the *EBNA1* region of p220.2 (29) was used as substrate. The sequence of the PCR primers were 5′-biotin-TCATGCCATC-CGTAAGATGC-3′ and 5′-CTGGTTGCTCCCATTCTTAG-3′. The methylation reaction mix contained 33 nM Dnmt3a, a given amount of TDG or Dnmt3L (33 nM) or HP1 (33 nM), 4 μg/ml of DNA, and 5.3 μM *S*-[methyl-^{3}H] Ado-Met (15 Ci/mmol; Amersham Biosciences) in a total volume of 25 μl with a reaction buffer comprising 20 mM HEPES (pH 7.5), 1 mM EDTA and 0.2 mM DTT. The reaction was incubated at 37°C for up to 60 min before scintillation

counts were measured. The methylation activity of M.SssI and M.HhaI were measured using the same method.

In vivo DNA methylation assay

In vivo methylation activity of Dnmt3a was assessed as described (29). A total of 0.5 μg of the episomal assay plasmid p220.2 were co-transfected into 293 c18 cells in 35 mm dishes in combination with Dnmt3a and TDG constructs. Cells were replated into 100 mm dishes after 2 days. An aliquot of cells was used to confirm the expression of the transfected proteins by western analysis. The p220.2 plasmid was recovered from the transfected cells and digested with HhaI. The digestion pattern was analyzed by Southern hybridization using a ^{32}P-labeled probe derived from the *EBNA1* region of p220.2.

Avidin-biotin coupled DNA binding (ABCD) assay

The DNA binding capacity of TDG and Dnmt3a *in vitro* was assessed as described previously (30). Approximately 10 pmol of biotin labeled G/T or G/C oligoduplexes (the sequence is the same as used in the immunofluorescence assay) were incubated with 300 ng of purified recombinant proteins in the presence of 50 pmol unlabeled G/C oligoduplexes at 4°C for 1 h in ABCD buffer [50 mM Tris–HCl (pH 7.9), 150 mM NaCl, 10% glycerol, 5 mM $MgCl_2$, 0.1% NP-40, 0.1% CHAPS and 0.5 mM DTT], then 10 μl streptavidin-coated Sepharose beads (Amersham Biosciences) were added and the mixture was rotated at 4°C for 30 min. Precipitates were collected and washed four times with the ABCD buffer. Proteins in the precipitates were analyzed by standard western blotting.

RESULTS

TDG interacts directly with Dnmt3a

In an attempt to identify regulatory factors for DNA methylation, we searched for interaction partners of Dnmt3a by using yeast two-hybrid screening. From a mouse testis library of 7×10^6 transformants, five positive clones were isolated and characterized as encoding TDG.

The interaction between Dnmt3a and TDG was verified by a GST pull-down assay. Recombinant 6xHis-Dnmt3a and GST–TDG purified from *E.coli* were used. As shown in Figure 1A, a significant amount of Dnmt3a (~6% of the input) was co-precipitated with GST–TDG (Figure 1A, lane 3) but not with GST alone (lane 2). This result shows a direct interaction of the two proteins *in vitro*. The possibility of false positive interaction mediated by contaminating nucleic acids was eliminated by including micrococcal nuclease treatment in the GST pull-down assay: results were identical with or without this step, and a control for the digestion is also shown (Figure 1A, right panel).

To examine the interaction between Dnmt3a and TDG *in vivo*, we prepared mammalian expression constructs encoding epitope-tagged proteins for a co-immunoprecipitation assay. Whole extracts from 293T cells transfected with HA-Dnmt3a and Flag-TDG were immunoprecipitated with an anti-Flag antibody. Western analysis revealed that HA-Dnmt3a was immunoprecipitated in the presence of Flag-TDG (Figure 1B, lane 4). The co-immunoprecipitation

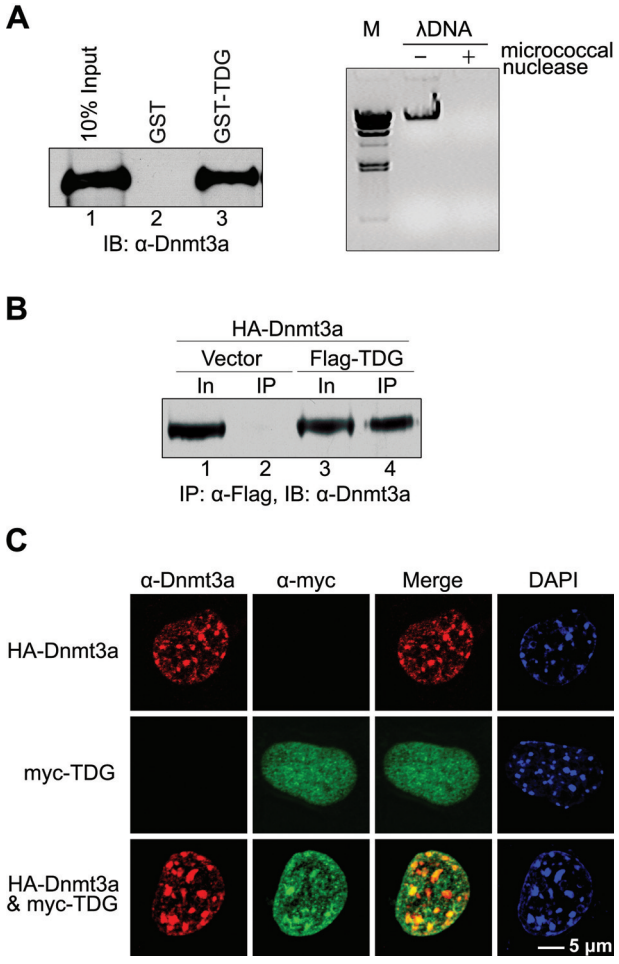

Figure 1. Dnmt3a interacts with TDG *in vitro* and *in vivo*. (**A**) Direct interaction of Dnmt3a with TDG. Western analysis of the recombinant Dnmt3a in fractions obtained from a GST pull-down assay using GST (lane 2) or GST–TDG (lane 3). 10% of the input Dnmt3a was loaded (lane 1). IB: antibody used for immunoblotting. Removal of any contaminating DNA from the protein samples prior to the pull-down experiment was verified by examining a sample spiked with λ DNA (100 ng/μl) on an agarose gel after the micrococcal nuclease digestion step (right panel). (**B**) Co-immunoprecipitation of transfected Dnmt3a with TDG from 293T cells. Western analysis of HA-Dnmt3a in whole cell extract (In) (lanes 1 and 3 with 10% of the input loaded) and immunoprecipitates (IP) obtained with anti-Flag antibody from extracts of cells transfected with HA-Dnmt3a and empty Flag vector (lane 2) or Flag-TDG expression construct (lane 4). (**C**) Nuclear co-localization of transfected HA-Dnmt3a (red) and myc-TDG (green) in NIH 3T3 cells. Fluorescence immunostaining of cells expressing either myc-TDG, HA-Dnmt3a or both was performed using the antibodies indicated on top. Merge of the double stained images allows assessment of the degree of co-localization of nuclear foci. DAPI counter-staining defines the nuclear territory including heterochromatin domains.

was specific because no signal was detected from the cell extract without Flag-TDG (lane 2). These data indicate that the two proteins can form a complex in transfected cells.

We then examined the distribution of co-transfected HA-Dnmt3a and myc-TDG in 3T3 cells. As expected, Dnmt3a displayed a diffuse nuclear pattern with discrete intense spots largely overlapping with heterochromatin domains defined by bright DAPI staining in >80% of cells, whereas only diffuse nuclear staining was observed with myc-TDG (Figure 1C). We consistently observed that co-expression of HA-Dnmt3a and myc-TDG resulted in a change of the

distribution pattern of myc-TDG, which became concentrated in the heterochromatin domains where HA-Dnmt3a was located in the majority of co-transfected cells (over 60%).

To further investigate whether Dnmt3a can be targeted to a G/T mismatched site, a fluorescently-labeled DNA duplex containing a single G/T mismatch was transfected into 3T3 cells together with myc-TDG and HA-Dnmt3a. Signal from the G/T mismatch-containing oligoduplexes appeared strongly in the nucleus and weakly in the cytoplasm (Figure 2A), consistent with previous observations with transfected DNA (31). Dnmt3a was mainly located in the nucleus when co-transfected with the mismatched oligo. However, it became distributed throughout the whole cell (in over 80% of cells) when co-transfected with both the G/T mismatch oligo and TDG (4th row). In contrast, both TDG and Dnmt3a remained nuclear when a control matched oligo was used (last row). Therefore, Dnmt3a is recruited to the cytoplasm in the presence of TDG and G/T mismatch-containing oligoduplexes. Although repair does not occur in the cytoplasm in normal cells, these data nevertheless indicate that Dnmt3a can be recruited to G/T mismatch sites through its association with TDG. The avidin–biotin coupled DNA binding assay (Figure 2B) further suggests a sequential binding of TDG and Dnmt3a onto G/T oligoduplexes.

Interaction domains of Dnmt3a and TDG

Dnmt3a has a catalytic domain at the C-terminus, fused to a long regulatory region including a conserved PWWP domain, a PHD domain and an N-terminal part of ~250 amino acids

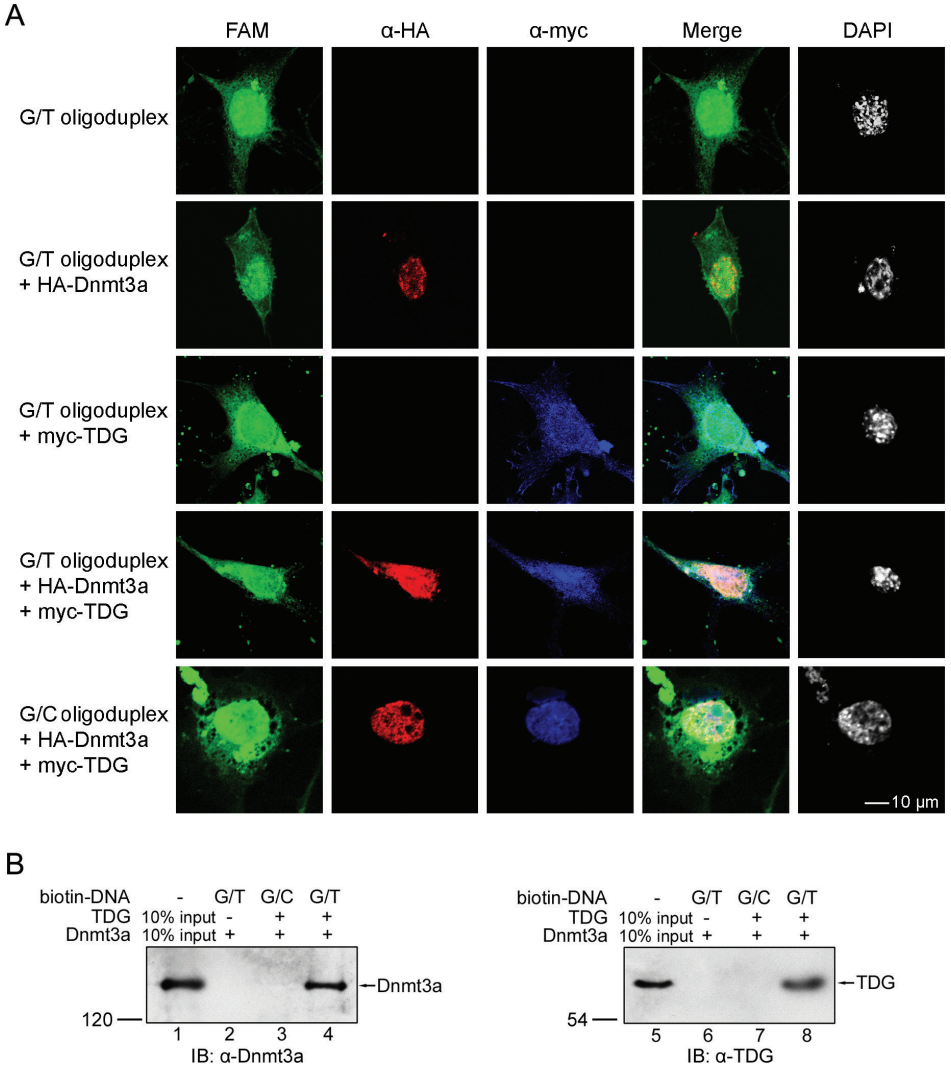

Figure 2. (**A**) TDG recruits Dnmt3a to oligos containing G/T mismatches *in vivo*. Co-localization of the transfected FAM-labeled G/T mismatch-containing DNA oligoduplexes (green), HA-Dnmt3a (red) and myc-TDG (pseudo-colored blue) in NIH 3T3 cells is shown. 300 pmol of DNA oligoduplexes were transfected into 3T3 cells grown in a 35 mm-dish either alone or with HA-Dnmt3a (1 μg), myc-TDG (1 μg), or a combination. Fluorescence imaging of transfected cells was performed by immunostaining using antibodies and FAM detection as indicated on the top. Merge of the images from the three left columns allows assessment of the degree of co-localization. DAPI counter-staining (pseudo-colored white) defines the nuclear territory including heterochromatin domains. Results shown are representative of three independent experiments. (**B**) Purified recombinant Dnmt3a binds to G/T mismatch-containing DNA oligoduplexes via the association with recombinant TDG. An avidin–biotin coupled DNA binding (ABCD) assay (see Materials and Methods) was performed with biotinylated G/T or G/C oligoduplexes and recombinant Dnmt3a alone or with TDG. The precipitates pulled down by the oligoduplexes were analyzed by western blotting.

lacking sequence conservation [(32) and Figure 3A]. The PWWP domain is responsible for targeting the enzyme to heterochromatin in the nucleus (23,33) and the PHD domain mediates interaction with histone deacetylase (34).

To map the TDG-interacting domain of Dnmt3a, a deletion analysis was performed using a yeast two-hybrid assay. Fragments of Dnmt3a were expressed as fusion proteins with GAL4DB domain and tested for interaction with TDG fused with the GAL4 activation domain. Yeast expressing either the PWWP (270–430 amino acid) or catalytic domains (592–908 amino acid) could grow on the selective medium lacking His, Leu, Trp and adenine (Figure 3A), but neither the N-terminal part nor PHD domain endowed growth potential. Therefore, Dnmt3a appears to encompass two separate regions, the PWWP domain and the catalytic domain, either of which alone is sufficient for mediating the interaction with TDG. The TDG-interacting capacity of the two regions was confirmed by GST pull-down assay (Figure 3B).

TDG is a monofunctional glycosylase with the conserved catalytic domain spanning the major length of the protein (Figure 3C). While a region from 99 to 347 amino acid encodes the G/U glycosylase activity, an additional N-terminal sequence of 43–98 amino acid is required to process G/T mismatches (18,35). To map the interaction domain in TDG, GST pull-down assays were performed using the recombinant GST–Dnmt3a fusion protein and ^{35}S-labeled TDG fragments synthesized *in vitro*. As shown in Figure 3C, all five fragments from the N-terminal half of TDG were able to bind to Dnmt3a, while the C-terminal region (198–397 amino acid) failed to do so. The N-terminal half contains at least two subdomains (1–52 and 121–205 amino acid), both of which can mediate interaction with Dnmt3a individually. Yeast two-hybrid assay confirmed the Dnmt3a-interacting capacity of the regions from the N-terminal half of TDG (Figure 3D).

Dnmt3a stimulates the glycosylase activity of TDG

Since the interaction of Dnmt3a and TDG involves their respective catalytic domains, we wanted to know whether they could functionally modulate each other's enzymatic activity. To this end, the glycosylase activity of TDG was measured in the presence and absence of purified Dnmt3a. We first expressed and purified recombinant His-tagged Dnmt3a and TDG from *E.coli*, and prepared a ^{32}P-labeled oligonucleotide duplex containing a G/T mismatch as substrate (Figure 4A). APE, an endonuclease known to stimulate the TDG activity, was also purified and used for comparison.

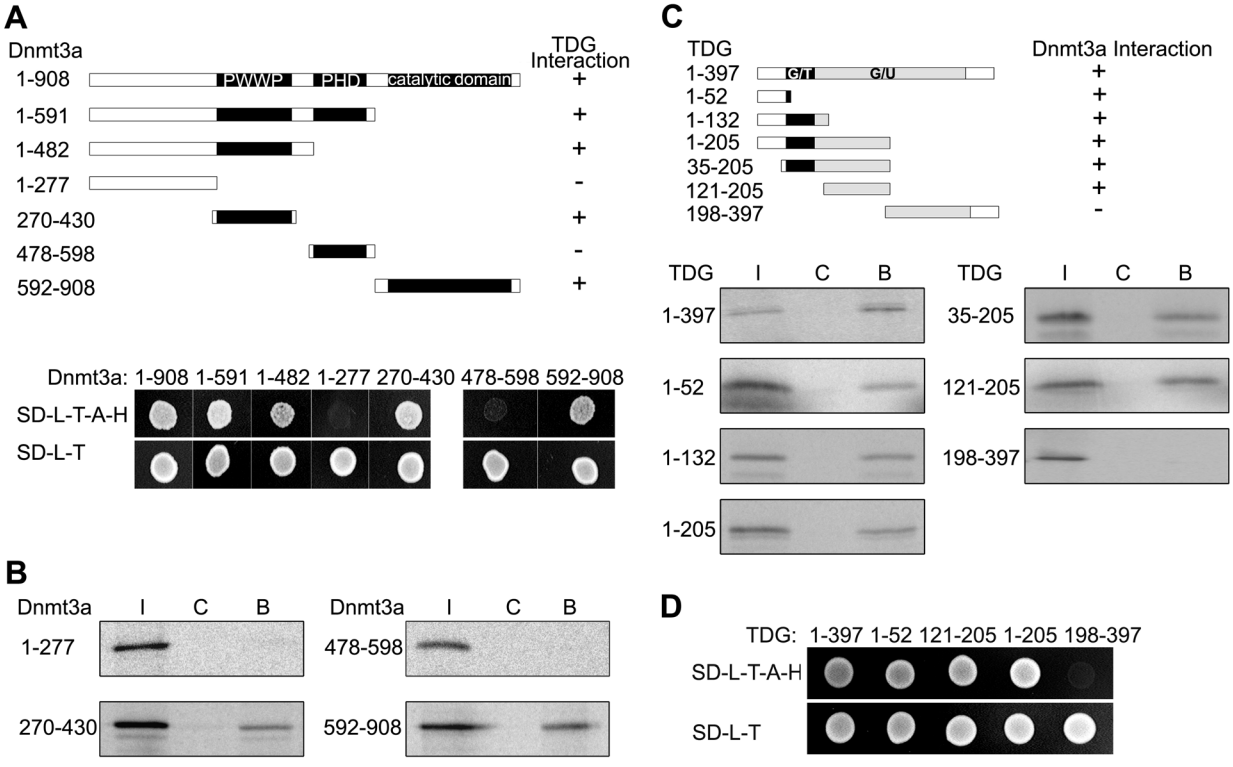

Figure 3. Mapping of Dnmt3a-TDG interaction domains. (**A**) Schematic representation of Dnmt3a fragments with their TDG-interacting abilities (shown on the right) based on the data from yeast two-hybrid assays (lower panel). Coordinates of the first and last amino acids of each Dnmt3a construct are given at the left. Yeast strain AH109 was co-transformed with a full-length TDG prey construct (GAL4AD fusion) and a bait construct (GAL4DB fusion) containing a Dnmt3a fragment from different regions. Growth of colonies on the SD minimal media lacking leucine, trypsine, adenine and histidine (SD-L-T-A-H) reflects positive interaction of a Dnmt3a fragment with TDG. (**B**) The binding abilities of *in vitro* translated, ^{35}S-labeled Dnmt3a fragments assessed by GST pull-down assay. I, 10% of input Dnmt3a fragments; C, bound fractions from the GST control; B, bound fractions from the GST–TDG fusion. (**C**) Schematic representation of TDG fragments with their Dnmt3a-interacting abilities (shown on the right) based on the data from GST pull-down assays (lower panel). The binding ability of *in vitro* translated, ^{35}S-labeled TDG fragment was tested with a GST–Dnmt3a fusion. I, 10% of input TDG fragments; C, bound fractions from the GST control; B, bound fractions from the GST–Dnmt3a fusion. (**D**) Confirmation of the N-terminal interacting regions of TDG using yeast two-hybrid assay. Yeast strain AH109 containing the full-length Dnmt3a bait construct and three N-terminal fragments of TDG prey constructs could grow on the SD minimal media (SD-L-T-A-H).

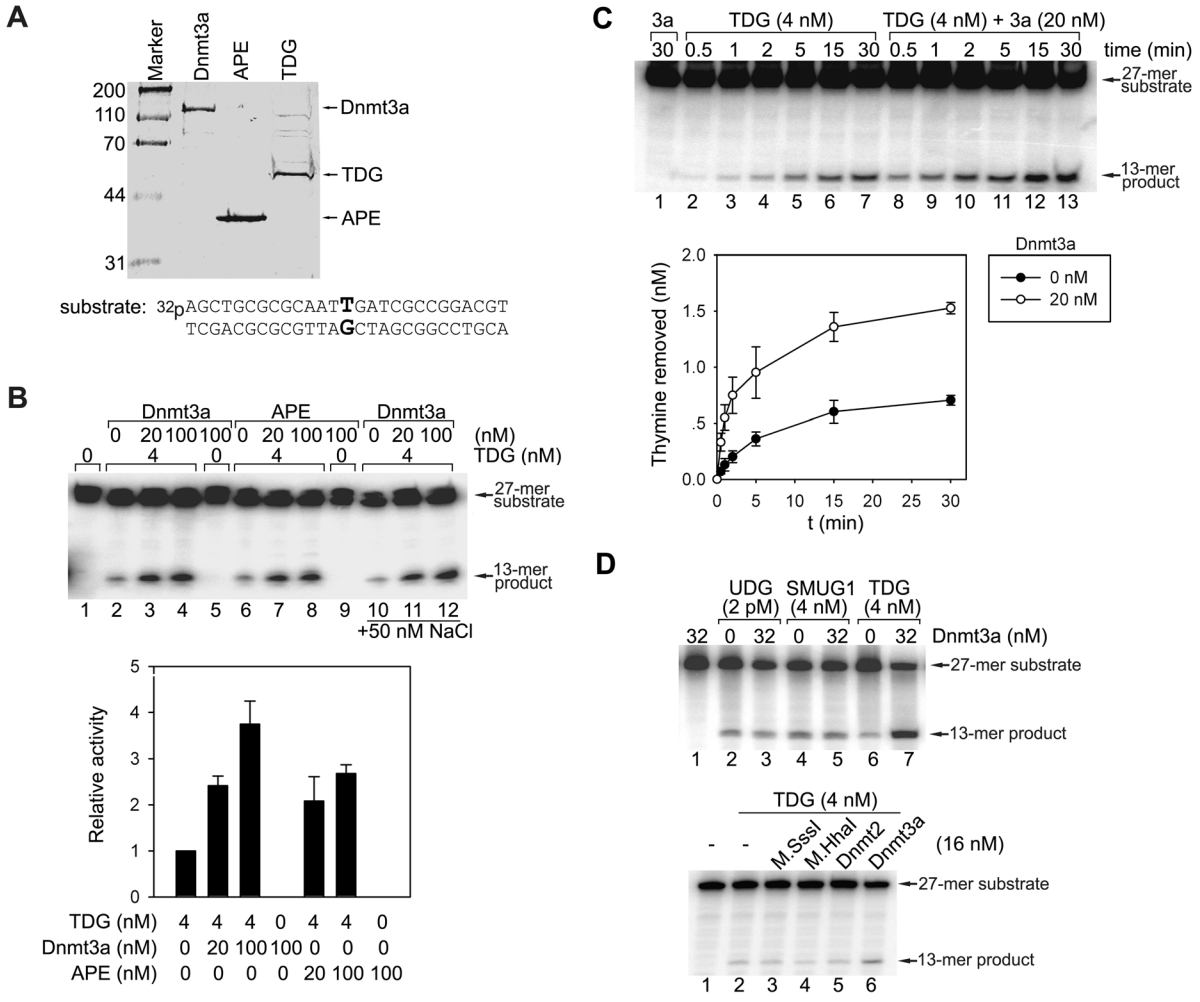

Figure 4. Dnmt3a stimulates the glycosylase activity of TDG. (**A**) Purified recombinant 6xHis-tagged Dnmt3a, APE and TDG proteins (Coomassie blue staining). The purity of Dnmt3a, APE and TDG was about 85, 90 and 80%, respectively, as determined by densitometry. Lower panel, the G/T mismatch-containing substrate (27 bp) used for the glycosylase activity assay. The upper T-containing strand was labeled with ^{32}P at the 5′ end. (**B**) Glycosylase activity assay for TDG in the absence and presence of Dnmt3a or APE. The reactions in lanes 1–9 contained 25 mM HEPES (pH 7.8), 0.5 mM EDTA, 0.5 mM DTT, 0.5 mg/ml BSA and 10 nM substrate DNA. The reactions in lanes 10–12 contained 50 mM NaCl and 2 mM $MgCl_2$ in addition to the above and show no difference, ruling out any possibility that the stimulation is only due to the addition of salt from the Dnmt3a prep. All reactions were incubated at 30°C for 1 h. The excision of unpaired thymine resulted in breakage of the upper strand upon subsequent hot alkaline treatment. The generation of the 13mer breakage product was examined by separation on a denaturing gel followed by quantification with phosphoimaging. The lower panel is a bar graph representation of TDG enzymatic assays. The activity of TDG alone was set to 1. The relative activity (given on the *y*-axis) for each reaction is the average of three experiments ±SD. (**C**) The kinetics of the base-excision reaction of TDG with and without Dnmt3a. DNA substrate (10 nM) was incubated with TDG (4 nM) alone or with Dnmt3a (20 nM) in the reaction buffer without NaCl for different time periods indicated on the top. The lower panel is a line graph representation in which the activity for each reaction at different time points is the average of three experiments ±SD. (**D**) Specific stimulation of TDG glycosylase activity by Dnmt3a. The glycosylase reaction was carried out for 30 min at 30°C. The upper panel shows the lack of stimulation of two other glycosylases UDG and SMUG1 by Dnmt3a. The DNA substrate used here had the same sequence as shown in (A) except that a G/U mismatch was incorporated in the place of G/T. The lower panel shows the absence of stimulation by M.SssI, M.HhaI and Dnmt2 on the glycosylase activity of TDG.

The glycosylase activity assay is based on the fact that the excision of mismatched thymine by TDG leaves an abasic site where the DNA strand breaks under hot alkaline treatment. As shown in Figure 4B, the amount of a 13mer break-down product increased when Dnmt3a was included in the reaction. Addition of 20 nM Dnmt3a resulted in a stimulation of TDG activity by 2.5-fold on average (Figure 4B, compare lanes 3 and 2), and 100 nM Dnmt3a brought about a stimulation of 3.8-fold (Figure 4B, compare lanes 4 and 2) under standard conditions reported previously (18). Moreover, the stimulatory effect appeared to be slightly stronger than that of APE (lanes 6 and 7). The fold stimulation by APE was consistent with previously reported data (21,27). We have also observed that purified Dnmt3a alone showed no detectable glycosylase activity, ruling out the possibility of contamination with a potent bacterial glycosylase in the Dnmt3a preparation (Figure 4B, lane 5). The reactions containing less than 100 nM Dnmt3a were made up to a similar volume with protein storage buffer, ensuring that the stimulatory effects were not due to alteration of salt or glycerol concentration. In addition, a similar degree of stimulation by Dnmt3a was also observed using a different reaction buffer containing 50 mM NaCl (27) (Figure 4B, lanes 11 and 12), ruling out any effects which might be due to salt in the preps.

Since the TDG activity in Figure 4B was measured after 60 min of incubation, we next asked whether the stimulation of TDG by Dnmt3a could also occur in the initial phase of the reaction. Consistent with previous work (27), a fast initial reaction was seen in the first 5 min in the absence of Dnmt3a (Figure 4C). With the addition of 20 nM Dnmt3a, the reaction was accelerated by 2- to 4-fold as calculated from the measurements at the time points of 0.5, 1, 2 and 5 min. This observation suggests that the interaction with Dnmt3a may facilitate the binding of the TDG enzyme with the mismatch substrate and/or excision of the thymine.

To further examine whether the stimulation by Dnmt3a is specific for TDG, we tested its effect on other glycosylases, the *E.coli* uracil DNA glycosylase (UDG) and its human homologue SMUG1. The glycosylase activity assay was conducted using the same DNA fragment (Figure 4A) but containing a G/U mismatch instead of G/T. We found that Dnmt3a had no effect on the activity of UDG and SMUG1 (Figure 4D, upper panel, lanes 2–5), while it stimulated the G/U activity of TDG (Figure 4D, upper panel, lanes 6 and 7). Moreover, the mouse DNA methyltransferase homologue Dnmt2 and bacterial methyltransferases M.SssI and M.HhaI did not stimulate the TDG activity (Figure 4D, lower panel). Taken together, these results indicate that Dnmt3a specifically stimulates the catalytic activity of TDG.

It should be noted that the specific activity (0.05–0.3 mol/h/mol enzyme) of our TDG enzyme preparation was similar to that reported by several other labs (18,27,30) but about 3- to 15-fold lower than that reported by Waters *et al*. (21). It is likely that a significant fraction of TDG molecules were inactive, potentially due to protein misfolding. Therefore, we could not formally exclude the possibility that Dnmt3a may also stimulate TDG activity through promoting conversion of its inactive form into the active form. Nevertheless, the stimulatory effect of Dnmt3a, though to varying degrees, has been consistently observed for multiple batches of TDG enzyme (with different purity and specific basal activity) obtained with the same or slightly modified chromatography steps. Furthermore, absence of effect by Dnmt2 or a bacterial methyltransferase suggests that stimulation of TDG activity depends on a specific interaction with Dnmt3a.

TDG represses the methylation activity of Dnmt3a

Since the Dnmt3a-TDG interaction involves the catalytic domain of Dnmt3a, we next investigated whether TDG has any effect on the methylation activity of Dnmt3a. The *in vitro* methylation activity of Dnmt3a was measured by scintillation-counting of the incorporation of a ^{3}H-labeled methyl group into a PCR fragment in reactions with or without TDG. As shown in Figure 5, the methyltransferase activity of Dnmt3a decreased in a dose-dependent manner. Incubating with an equimolar amount of TDG (33 nM) resulted in a reduction of Dnmt3a activity by 44% after 60 min, compared to the reaction without TDG (Figure 5A). When TDG was in 2-fold excess (100 nM) over Dnmt3a, this reduced the rate of methyl transfer by 78%. TDG and other proteins were dialyzed in buffer without salt prior to the assay as it is known that Dnmt3a is sensitive to the NaCl concentration. The reactions with no TDG contained a similar volume of the dialysis buffer, ensuring that the inhibition was not due to any residual salt or glycerol present in the TDG enzyme preparation.

To confirm the inhibition of the Dnmt3a activity by TDG is specific, we tested the effect of other known Dnmt3a interaction partners on methylation. Dnmt3L is a general stimulatory factor for the two Dnmt3 *de novo* methyltransferases and is essential for the establishment of genomic methylation patterns during germ cell development (36,37). Dnmt3L also interacts with Dnmt3a through the catalytic domain (38). As expected, the incubation with an equimolar amount of Dnmt3L resulted in a 120% increase of the Dnmt3a activity (Figure 5B). In contrast, the heterochromatin protein HP1, which is known to interact with the PHD domain of Dnmt3a, had no effect on the methylation activity (Figure 5B). We also tested the effect of TDG, if any, on two bacterial methyltransferases, M.SssI and M.HhaI. In both cases, no significant change in methylation activity was caused by the addition of TDG (Figure 5C). These data demonstrate that TDG functions as a repressor of Dnmt3a *in vitro,* although the exact molecular mechanism for the repression by TDG remains to be resolved. Presumably, TDG, but not HP1, may have an effect on the large mammalian enzyme by sterically hindering its binding to the DNA target.

Having shown the inhibitory effect of TDG on the activity of Dnmt3a *in vitro*, we then examined if TDG functions as a negative regulator of Dnmt3a *in vivo*. An episomal plasmid was transfected into 293 c18 cells with Dnmt3a and TDG constructs in varying amounts. The recovered plasmid was digested with the methylation-sensitive enzyme HhaI and Southern hybridization was carried out with a probe specific for the episomal plasmid. Three fragments of 1707, 738 and 189 bp would arise from the complete digestion when no methylation occurred; fragments of increased sizes show *de novo* methylation. As shown in Figure 5D, the fraction of larger-size fragments decreased when Dnmt3a was co-transfected with TDG (compare lanes 3 with 2). And when the amount of transfected TDG construct was increased by 1- and 2-fold, the fraction of fragments of increased sizes decreased further (Figure 5D, lanes 4, 5 and 7). This result shows that TDG can inhibit the activity of Dnmt3a *in vivo*.

DISCUSSION

In the present study, we have shown that Dnmt3a can interact with TDG both *in vitro* and *in vivo* and have mapped the interaction domains in each protein. Both the PWWP domain and the catalytic domain of Dnmt3a are able to mediate the interaction with TDG at its N-terminus. The interaction mutually affects their respective enzyme activities: Dnmt3a stimulates the glycosylase activity of TDG while TDG represses the methylation activity of Dnmt3a. These results provide evidence for a possible coupling of cytosine methylation with the base-excision repair pathway.

Methylcytosines undergo spontaneous deamination at a much higher rate than cytosines (39). The severity of the mutagenic threat posed by methylcytosine deamination is reflected in the existence of CpG islands in mammalian genomes, which are believed to arise due to the depletion of methylated CpG dinucleotides in the bulk of the genome

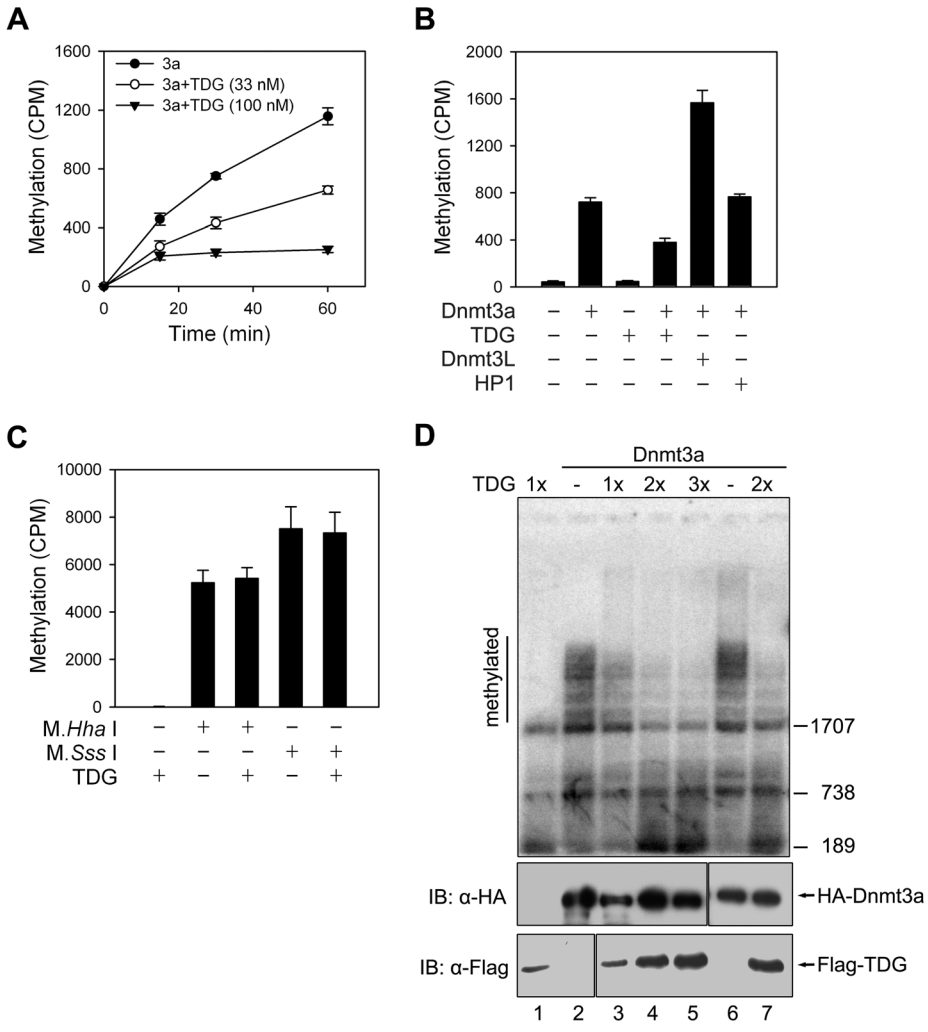

Figure 5. TDG represses the methylation activity of Dnmt3a. (**A**) Reduced methylation activity of Dnmt3a in the presence of TDG. The incorporation of a tritium-labeled methyl group into substrate DNA fragments was measured in CPM at three different time points, 15, 30 and 60 min. (**B**) The inhibitory effect of TDG on DNA methylation compared with other Dnmt3a-interacting proteins. Methylation reactions were carried out for 30 min with 33 nM Dnmt3a in the absence or presence of same molar amounts of TDG, Dnmt3L or HP1. (**C**) Absence of inhibitory effect of TDG on the activity of M.HhaI and M.SssI methyltransferases. The concentration used for each protein was 40 nM and the methylation reactions were carried out for 30 min. (**D**) The repression of *in vivo* methylation activity of Dnmt3a by co-transfected TDG. A total of 0.5 μg of the assay plasmid p220.2 was co-transfected with different combinations of Dnmt3a and TDG constructs (indicated on the top). The amount of Dnmt3a construct transfected was 0.5 μg. The amount of TDG construct ranged from 0.5 (1×) to 1.5 μg (3×). The methylation status of the recovered assay plasmid was analyzed by digestion with the methylation-sensitive enzyme HhaI followed by Southern hybridization. The two lower panels show the expression of Dnmt3a and TDG proteins, respectively. Results shown in (**A–C**) are from at least three independent experiments. Results in (**D**) are representative of two independent experiments.

during evolution (11). The mutagenic consequence is also evident in the fact that mC to T conversions account for one-third of the mutations found in the tumor suppressor gene p53 and other human disease genes (14,15,40). Mammals, like other organisms (41), have evolved mechanisms to counteract the mutagenic effect of methylcytosines. Of the eight mammalian glycosylases, TDG and MBD4 are the two enzymes that specialize in the correction of thymines in G/T mismatches to cytosines (16,42). TDG and MBD4 show very similar catalytic specificity in the excision of G/T mismatches in the CpG context, although their genes appear to be unrelated. The role of MBD4 in the elimination of deamination products in the context of a CpG dinucleotide has been confirmed in animal models (43,44).

However, the consequences of methylcytosine deamination are not confined to mutations. Even when the mC→T transition can be efficiently repaired back to cytosine, deamination itself still could have a profound impact on genome stability and gene expression. Both the restored cytosine at the mismatch site and those other newly-incorporated cytosines in the short-patch around it which are replaced by the action of the BER pathway need to be remethylated prior to the onset of DNA replication. If hemimethylated CpG sites in the repaired region are not converted into fully methylated sites, passive demethylation will occur after subsequent cell divisions. Our finding that Dnmt3a interacts with TDG, but not UDG, a uracil glycosylase which deals with the excision repair of cytosine deamination products, lends support to the idea that there is a need for remethylation of cytosines repaired from deaminated methylcytosines.

Our data show that TDG and Dnmt3a interact *in vitro* and that overexpression of Dnmt3a causes a significant change of

TDG localization (Figure 1C), suggesting it also interacts with Dnmt3a *in vivo*. Although co-localization has been consistently seen in several independent experiments, the overlap is only partial: one possible explanation is that the interaction with Dnmt3a is affected by post-translational modification of TDG such as sumoylation (45) or it may reflect the experimental noise often seen when using co-transfected proteins. It is known that mismatched G/T is recognized by either TDG or MBD4, but transfected Dnmt3a seems to have a stronger inherent ability to localize to heterochromatin regions than transfected TDG. For the endogenous proteins interacting with other components of the repair pathway in a normal situation, the interaction domains may allow recruitment to occur in the other direction, with Dnmt3a recruited to the G/T mismatch site via interaction with either of the glycosylases. In support of this view, Dnmt3a can be recruited to the mismatch-containing oligoduplexes via association with TDG, which recognizes G/T mismatches (Figure 2).

Supporting a Dnmt3a-TDG interaction *in vivo*, Dnmt3a appears to enhance glycosylase activity *in vitro*, possibly by facilitating the binding of TDG to the mismatch substrate and/or cleavage of the mismatched thymine. In this phase, the repressive effect of TDG on Dnmt3a could prevent a faulty transfer of methyl groups to nearby sequences. Then the second BER step ensues with the binding of the free abasic site by the APE DNA endonuclease, which has a higher affinity than TDG to the abasic DNA. Upon dissociation of TDG from the abasic site, Dnmt3a could remain at the repair site through interaction with another BER component, LIG3, the last enzyme of the short-patch BER pathway. It is noteworthy that Dnmt3a associates with LIG3 with even higher affinity compared with TDG (Supplementary Figure 1; P. Zhou and Y. Li, unpublished data). Cytosine remethylation must occur after the completion of base-excision repair by BER proteins: at this stage, TDG has left the repair site. The repressive effect on Dnmt3a doesn't exist anymore and so the methyltransfer process can proceed. Factors affecting the BER pathway or post-translational modification of TDG by sumoylation and acetylation (30,46) may also play a role in the coordination of the repair and remethylation processes.

Dnmt3b also contains the conserved PWWP and catalytic domains shown to mediate the interaction of Dnmt3a with TDG. Yeast two-hybrid and GST pull-down assays confirmed the physical interaction between Dnmt3b and TDG. Dnmt3b can also stimulate the activity of TDG (data not shown). Thus the two *de novo* DNA methyltransferases may both participate in the restoration of methylation status in base-excision repair.

The remethylation of cytosines is conceivably needed in a variety of DNA repair events involving strand re-synthesis in a methylated genomic region. In agreement with this, Dnmt1 was recently found to be recruited to sites of DNA damages induced by irradiation (47). However, the remethylation of cytosines restored at G/T mismatch sites is unlikely to be achieved by Dnmt1 since its recruitment to the repair site depends on PCNA (47), which is absent from the polymerase β-dependent short-patch BER pathway predominantly operating at AP sites, which require incorporation of only a single nucleotide (48–50). Consistent with this view, no interaction could be detected between Dnmt1 and TDG or LIG3 (Supplementary Figure 2).

Failure to remethylate might be an important contributor to the genomic hypomethylation observed in various diseases including cancer. The assessment of the biological significance of cytosine remethylation in disease as well as in normal development requires further investigation under physiological conditions.

SUPPLEMENTARY DATA

Supplementary Data are available at NAR online.

ACKNOWLEDGEMENTS

The authors thank Dr G. Verdine for the pGEX-3X-hSMUG1 expression construct, Dr A. Jeltsch for pFASTBACHTc-Dnmt1 and pET28-Dnmt2, Dr K. Yamamoto for pGEX-2T-mHP1a, Dr K. Sugasawa for pET28-APE, Dr K. Caldecott for pET16BXH (XRCC1), Dr T. Lindahl for pET16BHIII (LIG3), Dr J. Christman for the method of transfection of fluorescent tagged oligodeoxyribonucleotides and Dr J. Zhou for discussions. Work in G.X.'s laboratory is supported by grants from the China NSF, the Ministry of Science and Technology of China (National Basic Research Program 2005CB522400), Shanghai Municipal Commission for Science and Technology, and the Max Planck Society. C.W.'s laboratory is supported by the BBSRC (BBS/B/07403), the Northern Ireland HPSS R&D office (RRG 6.7) and Action Cancer. Funding to pay the Open Access publication charges for this article was provided by the China NSF.

Conflict of interest statement. None declared.

REFERENCES

1. Li,E. (2002) Chromatin modification and epigenetic reprogramming in mammalian development. *Nature Rev. Genet*., **3**, 662–673.
2. Bestor,T.H. (2000) The DNA methyltransferases of mammals. *Hum. Mol. Genet*., **9**, 2395–2402.
3. Costello,J.F. and Vertino,P.M. (2002) Methylation matters: a new spin on maspin. *Nature Genet*., **31**, 123–124.
4. Bird,A.P. (1986) CpG-rich islands and the function of DNA methylation. *Nature*, **321**, 209–213.
5. Bird,A. (2002) DNA methylation patterns and epigenetic memory. *Genes Dev*., **16**, 6–21.
6. Reik,W., Kelsey,G. and Walter,J. (1999) Dissecting de novo methylation. *Nature Genet*., **23**, 380–382.
7. Jones,P.A. and Baylin,S.B. (2002) The fundamental role of epigenetic events in cancer. *Nature Rev. Genet*., **3**, 415–428.
8. Jaenisch,R. and Bird,A. (2003) Epigenetic regulation of gene expression: how the genome integrates intrinsic and environmental signals. *Nature Genet*., **33**, 245–254.
9. Egger,G., Liang,G., Aparicio,A. and Jones,P.A. (2004) Epigenetics in human disease and prospects for epigenetic therapy. *Nature*, **429**, 457–463.
10. Duncan,B.K. and Miller,J.H. (1980) Mutagenic deamination of cytosine residues in DNA. *Nature*, **287**, 560–561.
11. Sved,J. and Bird,A. (1990) The expected equilibrium of the CpG dinucleotide in vertebrate genomes under a mutation model. *Proc. Natl Acad. Sci. USA*, **87**, 4692–4696.
12. Cooper,D.N. and Youssoufian,H. (1988) The CpG dinucleotide and human genetic disease. *Hum. Genet*., **78**, 151–155.
13. Jones,P.A., Rideout,W.M.,3rd, Shen,J.C., Spruck,C.H. and Tsai,Y.C. (1992) Methylation, mutation and cancer. *Bioessays*, **14**, 33–36.

14. Walsh,C.P. and Xu,G.L. (2006) Cytosine methylation and DNA repair. *Curr. Top Microbiol. Immunol.*, **301**, 283–315.
15. Pfeifer,G.P. and Holmquist,G.P. (1997) Mutagenesis in the P53 gene. *Biochim. Biophys. Acta*, **1333**, M1–M8.
16. Hardeland,U., Bentele,M., Lettieri,T., Steinacher,R., Jiricny,J. and Schar,P. (2001) Thymine DNA glycosylase. *Prog. Nucleic Acid Res. Mol. Biol.*, **68**, 235–253.
17. Krokan,H.E., Drablos,F. and Slupphaug,G. (2002) Uracil in DNA--occurrence, consequences and repair. *Oncogene*, **21**, 8935–8948.
18. Neddermann,P., Gallinari,P., Lettieri,T., Schmid,D., Truong,O., Hsuan,J.J., Wiebauer,K. and Jiricny,J. (1996) Cloning and expression of human G/T mismatch-specific thymine-DNA glycosylase. *J. Biol. Chem.*, **271**, 12767–12774.
19. Hendrich,B., Hardeland,U., Ng,H.H., Jiricny,J. and Bird,A. (1999) The thymine glycosylase MBD4 can bind to the product of deamination at methylated CpG sites. *Nature*, **401**, 301–304.
20. Scharer,O.D. and Jiricny,J. (2001) Recent progress in the biology, chemistry and structural biology of DNA glycosylases. *Bioessays*, **23**, 270–281.
21. Waters,T.R., Gallinari,P., Jiricny,J. and Swann,P.F. (1999) Human thymine DNA glycosylase binds to apurinic sites in DNA but is displaced by human apurinic endonuclease 1. *J. Biol. Chem.*, **274**, 67–74.
22. Kastan,M.B., Gowans,B.J. and Lieberman,M.W. (1982) Methylation of deoxycytidine incorporated by excision-repair synthesis of DNA. *Cell*, **30**, 509–516.
23. Ge,Y.Z., Pu,M.T., Gowher,H., Wu,H.P., Ding,J.P., Jeltsch,A. and Xu,G.L. (2004) Chromatin targeting of *de novo* DNA methyltransferases by the PWWP domain. *J. Biol. Chem.*, **279**, 25447–25454.
24. Nguyen,T.N. and Goodrich,J.A. (2006) Protein–protein interaction assays: eliminating false positive interactions. *Nature Meth.*, **3**, 135–139.
25. Gowher,H. and Jeltsch,A. (2001) Enzymatic properties of recombinant Dnmt3a DNA methyltransferase from mouse: the enzyme modifies DNA in a non-processive manner and also methylates non-CpG [correction of non-CpA] sites. *J. Mol. Biol.*, **309**, 1201–1208.
26. Neddermann,P. and Jiricny,J. (1993) The purification of a mismatch-specific thymine-DNA glycosylase from HeLa cells. *J. Biol. Chem.*, **268**, 21218–21224.
27. Shimizu,Y., Iwai,S., Hanaoka,F. and Sugasawa,K. (2003) Xeroderma pigmentosum group C protein interacts physically and functionally with thymine DNA glycosylase. *EMBO J.*, **22**, 164–173.
28. Roth,M. and Jeltsch,A. (2000) Biotin-avidin microplate assay for the quantitative analysis of enzymatic methylation of DNA by DNA methyltransferases. *Biol. Chem.*, **381**, 269–272.
29. Xie,Z.H., Huang,Y.N., Chen,Z.X., Riggs,A.D., Ding,J.P., Gowher,H., Jeltsch,A., Sasaki,H., Hata,K. and Xu,G.L. (2006) Mutations in DNA methyltransferase DNMT3B in ICF syndrome affect its regulation by DNMT3L. *Hum. Mol. Genet.*, **15**, 1375–1385.
30. Tini,M., Benecke,A., Um,S.J., Torchia,J., Evans,R.M. and Chambon,P. (2002) Association of CBP/p300 acetylase and thymine DNA glycosylase links DNA repair and transcription. *Mol. Cell*, **9**, 265–277.
31. Nakamura,N., Hart,D.A., Frank,C.B., Marchuk,L.L., Shrive,N.G., Ota,N., Taira,K., Yoshikawa,H. and Kaneda,Y. (2001) Efficient transfer of intact oligonucleotides into the nucleus of ligament scar fibroblasts by HVJ-cationic liposomes is correlated with effective antisense gene inhibition. *J. Biochem. (Tokyo)*, **129**, 755–759.
32. Qiu,C., Sawada,K., Zhang,X. and Cheng,X. (2002) The PWWP domain of mammalian DNA methyltransferase Dnmt3b defines a new family of DNA-binding folds. *Nature Struct. Biol.*, **9**, 217–224.
33. Chen,T., Tsujimoto,N. and Li,E. (2004) The PWWP domain of Dnmt3a and Dnmt3b is required for directing DNA methylation to the major satellite repeats at pericentric heterochromatin. *Mol. Cell. Biol.*, **24**, 9048–9058.
34. Fuks,F., Burgers,W.A., Godin,N., Kasai,M. and Kouzarides,T. (2001) Dnmt3a binds deacetylases and is recruited by a sequence-specific repressor to silence transcription. *EMBO J.*, **20**, 2536–2544.
35. Gallinari,P. and Jiricny,J. (1996) A new class of uracil-DNA glycosylases related to human thymine-DNA glycosylase. *Nature*, **383**, 735–738.
36. Bourc'his,D. and Bestor,T.H. (2004) Meiotic catastrophe and retrotransposon reactivation in male germ cells lacking Dnmt3L. *Nature*, **431**, 96–99.
37. Bourc'his,D., Xu,G.L., Lin,C.S., Bollman,B. and Bestor,T.H. (2001) Dnmt3L and the establishment of maternal genomic imprints. *Science*, **294**, 2536–2539.
38. Suetake,I., Shinozaki,F., Miyagawa,J., Takeshima,H. and Tajima,S. (2004) DNMT3L stimulates the DNA methylation activity of Dnmt3a and Dnmt3b through a direct interaction. *J. Biol. Chem.*, **279**, 27816–27823.
39. Ehrlich,M., Norris,K.F., Wang,R.Y., Kuo,K.C. and Gehrke,C.W. (1986) DNA cytosine methylation and heat-induced deamination. *Biosci. Rep.*, **6**, 387–393.
40. Waters,T.R. and Swann,P.F. (2000) Thymine-DNA glycosylase and G to A transition mutations at CpG sites. *Mutat. Res.*, **462**, 137–147.
41. Bhagwat,A.S. and Lieb,M. (2002) Cooperation and competition in mismatch repair: very short-patch repair and methyl-directed mismatch repair in *Escherichia coli*. *Mol. Microbiol.*, **44**, 1421–1428.
42. Wood,R.D., Mitchell,M., Sgouros,J. and Lindahl,T. (2001) Human DNA repair genes. *Science*, **291**, 1284–1289.
43. Millar,C.B., Guy,J., Sansom,O.J., Selfridge,J., MacDougall,E., Hendrich,B., Keightley,P.D., Bishop,S.M., Clarke,A.R. and Bird,A. (2002) Enhanced CpG mutability and tumorigenesis in MBD4-deficient mice. *Science*, **297**, 403–405.
44. Wong,E., Yang,K., Kuraguchi,M., Werling,U., Avdievich,E., Fan,K., Fazzari,M., Jin,B., Brown,A.M., Lipkin,M. *et al.* (2002) Mbd4 inactivation increases Cright-arrowT transition mutations and promotes gastrointestinal tumor formation. *Proc. Natl Acad. Sci. USA*, **99**, 14937–14942.
45. Takahashi,H., Hatakeyama,S., Saitoh,H. and Nakayama,K.I. (2005) Noncovalent SUMO-1 binding activity of thymine DNA glycosylase (TDG) is required for its SUMO-1 modification and colocalization with the promyelocytic leukemia protein. *J. Biol. Chem.*, **280**, 5611–5621.
46. Hardeland,U., Steinacher,R., Jiricny,J. and Schar,P. (2002) Modification of the human thymine-DNA glycosylase by ubiquitin-like proteins facilitates enzymatic turnover. *EMBO J.*, **21**, 1456–1464.
47. Mortusewicz,O., Schermelleh,L., Walter,J., Cardoso,M.C. and Leonhardt,H. (2005) Recruitment of DNA methyltransferase I to DNA repair sites. *Proc. Natl Acad. Sci. USA*, **102**, 8905–8909.
48. Lindahl,T. and Wood,R.D. (1999) Quality control by DNA repair. *Science*, **286**, 1897–1905.
49. Klungland,A. and Lindahl,T. (1997) Second pathway for completion of human DNA base excision-repair: reconstitution with purified proteins and requirement for DNase IV (FEN1). *EMBO J.*, **16**, 3341–3348.
50. Nilsen,H. and Krokan,H.E. (2001) Base excision repair in a network of defence and tolerance. *Carcinogenesis*, **22**, 987–998.